SURFACE WARMING DURING THE 2018/MY 34 MARS GLOBAL DUST STORM. P. M. Streeter[1], S. R. Lewis[1], M. R. Patel[1,2], J. A. Holmes[1], and D. M. Kass[3], [1]School of Physical Sciences, The Open University, Walton Hall, Milton Keynes MK7 6AA, U.K. (paul.streeter@open.ac.uk), [2]Space Science and Technology Department, Science and Technology Facilities Council, Rutherford Appleton Laboratory, Harwell Campus, Didcot, Oxfordshire OX11 0QX, U.K., [3]Jet Propulsion Laboratory, California Institute of Technology, Pasadena, California, U.S.A.

Introduction:

Suspended atmospheric dust is a crucial active component of Mars' atmosphere, with significant radiative-dynamical effects through its scattering and absorption of radiation [2,14]. The exact nature of these effects depends on a variety of factors. Aerosol optical depth is important, as are the specific radiative properties of the aerosol particles [18]. Also important for surface and near-surface effects are the properties of the martian ground itself, and in particular albedo and surface thermal inertia (TI) [11].

Mars Global Dust Storms (GDS) are spectacular, planet-spanning events which act to dramatically increase dust opacities. The 2018 GDS was observed through its lifecycle by the Mars Climate Sounder (MCS) instrument aboard the Mars Reconnaissance Orbiter [16]; using data assimilation to integrate MCS observations with a Mars Global Circulation Model (MGCM) therefore offers an opportunity to examine the effects of the GDS on surface and near-surface temperatures (STs and NSTs), and the interplay between the factors described above. The reanalysis contains the MGCM's best possible representation of the GDS geographical and temporal structure.

Methods:

Model and assimilation details.

We used the UK version of the LMD MGCM [1,8,10], which possesses a spectral dynamical core and semi-Lagrangian advection scheme [13], and is a collaboration between the Laboratoire de Météorologie Dynamique, The Open University, the University of Oxford, and the Instituto de Astrofísica de Andalucía. Dust radiative properties are derived from observational studies, including of the 2007 GDS [19,20]. Dust is freely advected by the MGCM using a two-moment scheme with a log-normal size distribution [10] with total dust optical depths on each column scaled to match assimilated observations. The model was run at a spectral resolution of T42, corresponding to gridbox dimensions of ~3.75°, and 50 vertical levels from 5 m to 105 km. The model uses a surface TI map derived from Thermal Emission Spectrometer (TES) observations [15]. The assimilation scheme used was a modified version of the Met Office Analysis Correction scheme [9], adapted for Mars [8].

MCS observations.

The retrievals used in this study are from the Mars Climate Sounder (MCS) instrument aboard the Mars Reconnaissance Orbiter (MRO) [12]. The retrieved temperature profiles and dust columns were assimilated simultaneously. Temperature profiles extend from the surface to approximately 100 km altitude, and dust columns are derived from profiles from as low as 10 km above the surface up to a maximum height of approximately 50 km. The retrieval version used was 5.2, a re-processing using updated 2D geometry [7]. For the period of the GDS itself, the retrieval version used was 5.3.2.

Results:

We find that the 2018 GDS caused an increase in global average martian STs of 0.9 K relative to Mars Year (MY) 30, as averaged over all local times. The degree of dayside cooling at a location was determined by dust column optical depth, while that of nightside warming was determined by surface TI. The continents of lowest TI underwent diurnally-averaged warming, while higher TI regions underwent either no net change or a net cooling depending on the dust loading.

The martian dayside underwent up to 39 K cooling at the model resolution used, with a globally averaged value of 14 K. The greatest cooling occurred at Chryse, northern Hellas, Argyre, Isidis, and Amazonia (Fig. 1b). In general, areas of greatest cooling correlated with total dust column optical depth.

The nightside underwent warming of up to 42 K with globally average value 13 K. The greatest warming occurred at Tharsis, Elysium Mons, Amazonia, and Arabia (Fig. 1c), all regions of low TI despite spanning a range of elevations and dust loadings.

Areas of greatest cooling did not necessarily match those of greatest warming due to the differing mechanisms behind each effect; the diurnally averaged effect was therefore heterogenous, with some regions experiencing net warming, some net cooling, and some little change. The most visible diurnally averaged effect (Fig. 1a) was the pronounced surface warming of low TI continents between latitudes 20° S and 40° N, specifically Tharsis, Amazonia, Elysium Planitia and Elysium Mons, and Arabia Terra.

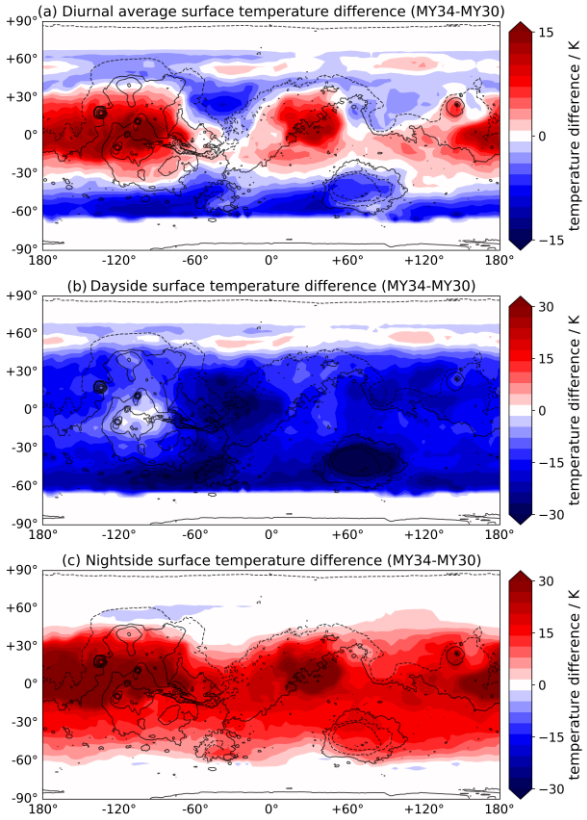

Fig. 1: Surface temperature difference between MY 34 and MY 30 for the period L_S = 200°-220°: (top) diurnally-averaged, (middle) at 1500, and (bottom) at 0300.

Globally and diurnally-averaged NSTs also increased, by 5.3 K. Nightside NST increases tracked nightside ST increases, with slightly lower magnitude. Dayside tropical NSTs actually increased relative to the clear case, due to the close ST-NST coupling induced by the high dust loading, which increased both SW and LW absorption in the near-surface atmosphere. (Dayside) locations where GDS-case STs were higher than clear-case NSTs therefore saw a NST increase.

The diurnal temperature cycles at specific locations of high and low TI but similar dust loadings were examined in greater detail; confirming that while both regions underwent similar dayside cooling, the magnitude of nightside warming was much greater at the low TI region. The GDS acted to reduce the amplitude of the diurnal temperature cycle by a factor of ~2.

Discussion:

The competing factors of surface TI and column dust loading drive surface nightside warming (from increased surface incident longwave flux) and dayside cooling (from decreased surface incident shortwave flux) respectively, with the overall effect of a globally- and diurnally-averaged warming of 2.1 K. This warming was geographically concentrated around low TI hotspots, where the usual rapid night-time surface cooling was inhibited by enhanced longwave flux.

Surface orbital data from GDS events is sparse, due to the difficulties of remote sensing under high dust loadings. However, the MY 25/2001 GDS provides some opportunity for validation. The TES instrument observed peak cooling/warming of 23 K/18 K at L_S = 210° [17], corresponding to a 2.5 K net cooling; a reanalysis of the MY 25 GDS [6] agrees with a 2.5 K decrease, based off cooling/warming of 20 K/18 K for the same period (note that this is averaged over two local times, not all local times; the latter gives a 0 K change). Radio telescope observations of dayside STs also agree with the magnitude of cooling, of ~20 K [3].

While the MGCM does not resolve Gale Crater, an analogue location with similar dust loading, insolation, and TI was analysed; a peak decrease/increase in surface temperatures of 24 K/19 K was predicted, corresponding to a net decrease of 2.5 K. Curiosity measured 21 K/14 K, net decrease 3.5 K [4]; the MGCM compares favourably but appears to overestimate dayside cooling and especially nightside warming. Further discussion will be presented.

Additionally, comparison of the MY34 and MY25 events suggests that the structure of GDS events, and specifically their coverage of low TI areas, has a significant impact on their overall ST effects.

References:

[1] Forget F. et al (1999) *JGR, 104*, 24155-24175. [2] Gierasch P. J. and Goody R. M. (1972) *J. Atmos. Sci., 29*(2), 400-402. [3] Gurwell M. A. et al (2005) *Icarus, 175*(1), 23-31. [4] Guzewich S. D. et al (2019) *GRL, 46*(1), 71-79. [5] Hanel R. et al (1972) *Icarus, 17*(2), 423-442. [6] Holmes J. A. et al (2019) [*OpenMars Fileset.]* [7] Kleinböhl A. et al (2017) *J. Quant. Spectrosc. Radiat. Transfer, 187*, 511-522. [8] Lewis S. R. et al (2007) *Icarus, 192*(2), 327-347. [9] Lorenc A. C. et al (1991) *QJRMS, 117*, 59-89. [10] Madeleine J.-B. et al (2011) *JGR (Planets), 116* (E11010). [11] Martínez G. M. et al (2017) *Space Science Reviews, 212*(1), 295-338. [12] McCleese D. J. et al (2010) *J. Geophys. Res., 115*(E12016). [13] Newman C. E. et al (2002) *JGR, 107*, 5123. [14] Pollack J. B. et al (1979) *JGR (Solid Earth), 84*(B6), 2929-2945. [15] Putzig N. E. et al (2005), *Icarus, 173*(2), 325-341. [16] Shirley J. H. et al (2018) *AGU Fall Meeting Abstracts 43*. [17] Smith M. D. (2004) *Icarus, 167*(1), 148-165. [18] Turco R. P. et al (1984) *Scientific American, 251*(2), 33-43. [19] Wolff M. J. et al (2006) *JGR (Planets), 111*(E12). [20] Wolff M. J. et al (2009) *JGR (Planets), 114*(E00D04).